

# 3D-SOULE: A FABRICATION PROCESS FOR LARGE SCALE INTEGRATION AND MICROMACHINING OF SPHERICAL STRUCTURES

Karthik Visvanathan<sup>1</sup>, Tao Li<sup>2</sup>, and Yogesh B. Gianchandani<sup>1,2</sup>

<sup>1</sup>Department of Mechanical Engineering, University of Michigan, Ann Arbor, USA

<sup>2</sup>Department of Electrical Engineering and Computer Science, University of Michigan, Ann Arbor, USA

## ABSTRACT

This paper reports a method for integrating and micromachining spherical structures made from materials such as fused quartz that are not amenable to melting or reflow. The 3D-SOULE process combines batch-mode micro ultrasonic machining ( $\mu$ USM), lapping, and micro electro-discharge machining ( $\mu$ EDM) for creating spherical structures. Micro electro discharge machining is used for creating the stainless steel tool, which is then used for  $\mu$ USM of the glass spheres. Stainless steel 440 which provides tool wear  $<5\%$  is used for  $\mu$ USM. A machining rate of  $24 \mu\text{m}/\text{sec}$  is achieved for fabrication of concave and mushroom-shaped spherical structures from 1 mm-diameter glass spheres.

## INTRODUCTION

Three dimensional (3D) microstructures in hemispheric, “wine glass” and mushroom shapes are attractive for certain types of inertial sensors (such as rate integrating gyroscopes) (Fig. 1) [1-3]. Most conventional surface and bulk microfabrication methods like etching, film deposition, photolithography, etc. are limited to creating planar structures. Microfabrication methods such as LIGA [4,5] and deep reactive ion etching (DRIE) [6,7] are well suited for creating high-aspect-ratio structures out of metal and silicon, respectively. However, these methods are not easily adapted for spherical shapes. The use of isotropic wet etching, deposition and oxidation to microfabricate free standing spherical structures from silicon dioxide is discussed in [8]. The fabrication of dome shaped structure utilizing the buckling of a prestressed thin polysilicon film is discussed in [9]. The thicknesses of the shells fabricated using these techniques are a few microns. Recently, a wafer-scale glass blowing process has been reported for the fabrication of spherical shells from glass composites that can melt at modest temperatures [10]. In this process cavities are etched into silicon, followed by anodic bonding of a glass wafer to the silicon wafer. The wafers are then heated above the softening-point temperature of the glass. The expansion of the trapped gas in the silicon cavities leads to formation of 3D spherical shells.

In this paper, we report a complementary method for integrating and micromachining concave and mushroom-shaped spherical structures made from materials such as fused quartz that are not amenable to melting or reflow. The 3D-SOULE process is a 3D-capable and self-aligned process combining batch-mode micro ultrasonic machining ( $\mu$ USM), lapping, and micro electro-discharge machining ( $\mu$ EDM). Since  $\mu$ USM does not involve any chemical or

high temperature steps, it is possible to create stress-free structures in a wide variety of ceramics, glasses and other brittle materials [11,12]. The following sections describe the fabrication process, fabrication results and the testing of the resonance characteristics of the fabricated structures.

## PROCESS DESCRIPTION

Figure 2 shows the schematic of the 3D-SOULE process for fabricating concave and mushroom-shaped spherical structures. Initially,  $\mu$ EDM is used to micromachine cavities in the steel substrate for holding stainless steel spheres (Fig. 2.1). In the  $\mu$ EDM process, the tungsten electrode and the stainless steel workpiece are immersed in dielectric oil (kerosene). A pulsed discharge is used to perform the machining. The stainless steel workpiece is eroded much faster during the discharge than the tungsten electrode.

Nonconductive epoxy is then applied into the cavities on the stainless steel substrate. Commercially-obtained stainless steel spheres of 0.8 mm diameter (A.F.B.M.A. grade 25), with high geometrical precision (sphericity  $<0.625 \mu\text{m}$ ), are then assembled into these cavities. The stainless steel spheres are then pressed into the epoxy from above using a flat substrate, after which the epoxy is then allowed to cure. This ensures that the tips of all the spheres are at the same level (Fig. 2.2). For the mushroom shape, an additional  $\mu$ EDM step is performed to form the cavities, of  $200 \mu\text{m}$  diameter and  $750 \mu\text{m}$  depth, at the center of the stainless steel spheres (Fig. 2.3b). This enables the formation of stems for the mushroom-shaped structures. The diameter of the cavities determines the diameter of the stem in the mushroom-shaped structure at the end of the process. The X-Y resolution of the  $\mu$ EDM positioning stage is  $0.1 \mu\text{m}$ , which enables the fabrication of stainless steel spheres with centered holes.

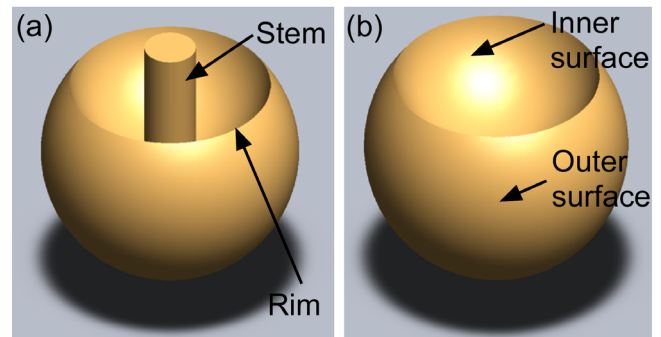


Figure 1: Schematic of the (a) Mushroom and (b) concave shaped spherical structure fabricated using the 3D-SOULE process.

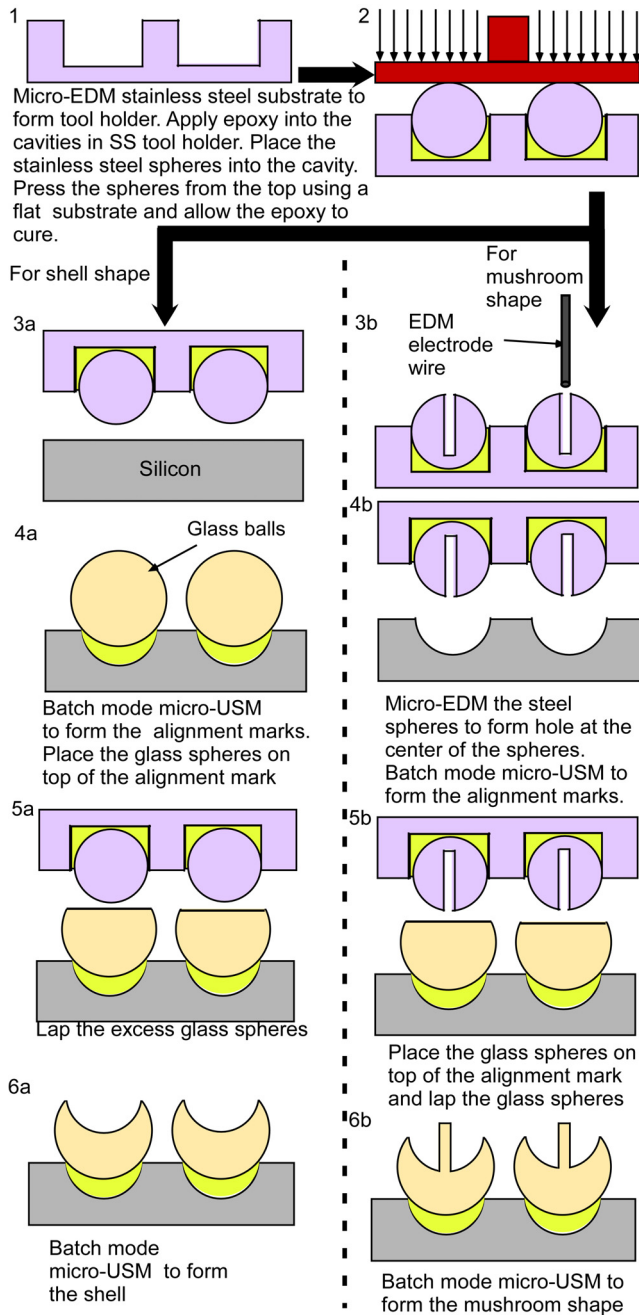


Figure 2: 3D-SOULE process diagram for fabrication of concave and mushroom-shaped spherical structures. 3D-SOULE process utilizes serial  $\mu$ EDM, batch mode  $\mu$ USM and lapping to fabricate devices in the above mentioned shapes. This process can be applied to a wide variety of glasses, fused quartz, etc.

Next a silicon carrier substrate is bonded to the glass plate. Batch-mode  $\mu$ USM [11,12] is then used to form alignment marks ( $100 \mu\text{m}$  deep) on the silicon carrier substrate with the above assembled stainless steel tool (Fig. 2.4b). In this process, a 20 kHz ultrasound generator with vibration amplitude of  $15 \mu\text{m}$  is used. This vibration, in turn, is transferred to fine abrasive particles that are suspended in water between the tool and the silicon

Table 1: Comparison of tool wear in SS 316 and SS 440 spheres during USM machining.

	SS316	SS440
Substrate machined	Glass	Glass
Depth of machining	$300 \mu\text{m}$	$300 \mu\text{m}$
Tool wear (volume)	$1.30 \times 10^{-11} \text{m}^3$	$3.68 \times 10^{-12} \text{m}^3$
Wear ratio (volume)	31.7%	4.46%

substrate. Tungsten carbide powder of  $0.5\text{-}1 \mu\text{m}$  particle size is used in this process. The pattern on the assembled tool is then transferred onto the silicon substrate by microchipping caused by the bombardment of the high speed powders. For the mushroom shape, an additional step is performed to remove the post formed at the center of the alignment mark.

Glass spheres of  $1 \text{mm}$  diameter (NBK7,  $1 \mu\text{m}$  sphericity) with high precision and surface finish are mounted and self-assembled into the indents created on the silicon substrate (Fig. 2.4a). This ensures that the center of the microtool and the target glass spheres are self-aligned to each other with high geometrical precision. The glass spheres are bonded to the silicon substrate using epoxy (Stycast 2850). Lapping is performed with  $0.25 \mu\text{m}$  diamond slurry to remove the excess epoxy and to reduce the height of the glass spheres as desired (Fig. 2.5a,b). A copper lapping plate is used in this process. Batch-mode  $\mu$ USM on the lapped glass spheres is then performed to form the desired structure (Fig. 2.6a,b). The  $\mu$ USM process leads to the formation of sharp edges along the rim of the fabricated structure. An additional lapping step can be performed in order to remove the sharp edges on the machined glass spheres. The glass spheres are finally released from the silicon substrate using Dynasolve 165.

## EXPERIMENTAL RESULTS

### Fabrication Results

Material wear during batch-mode  $\mu$ USM for stainless-steel spheres made of SS440 and SS316 were compared for determining the most suitable tool material for this application. Machining of the NBK-7 spheres was performed using SS316 and SS440 spheres and the tool wear was determined by measuring the change in the height of the sphere after machining. A laser displacement sensor (Keyence LKGD500) was used for measuring the wear on the stainless steel spheres. Table 1 lists the comparison of the wear in SS440 and SS316 spheres. Tool wear for SS440 was less than one-sixth as that of SS316. Hence SS440

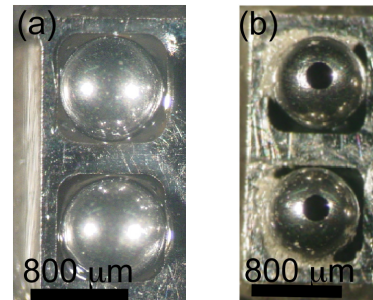


Figure 3: (a) USM tool for fabrication of spherical shell. (b) USM tool for fabrication of mushroom shaped structure with cavities at the center of the sphere.

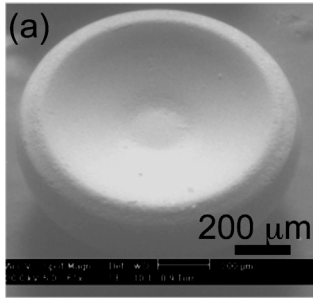
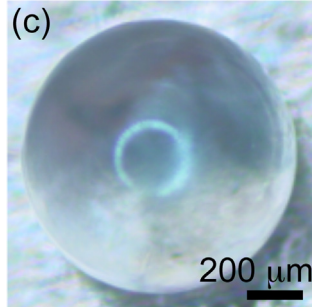
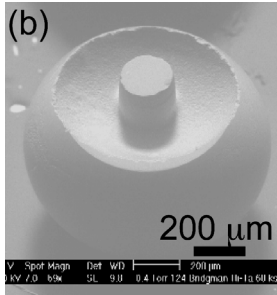


Figure 4: SEM image of the fabricated (a) concave spherical structure and (b) mushroom shaped structure. (c) Photograph of the top view of the mushroom structure made from transparent NBK7 glass spheres.



spheres were used in the fabrication process.

Figures 3a and 3b show the photograph of the assembled USM tool for fabrication of concave and mushroom-shaped spherical structures, respectively. Figures 4a and 4b show the SEM images of the fabricated concave and the mushroom-shaped spherical structures. The photograph of the outer surface of a mushroom structure is shown in Fig. 4c. The machining parameters for the batch mode  $\mu$ USM used in the 3D-SOULE process are listed in Table 2. A machining rate of  $24 \mu\text{m}/\text{sec}$  is achieved for a machining depth of  $350 \mu\text{m}$  at a vibration amplitude and frequency of  $15 \mu\text{m}$  and  $20 \text{ kHz}$ , respectively, of the ultrasound generator.

Table 2: Machining parameters for the batch mode USM in the 3D-SOULE process

Ultrasound generator frequency	20 kHz
Ultrasound vibration amplitude	$15 \mu\text{m}$
Abrasive powder (Tungsten carbide)	$0.5\text{-}1 \mu\text{m}$
Avg. machining rate (depth)	$24 \mu\text{m}/\text{sec}$
Machining load	0.5 N
Cutting depth	$350 \mu\text{m}$

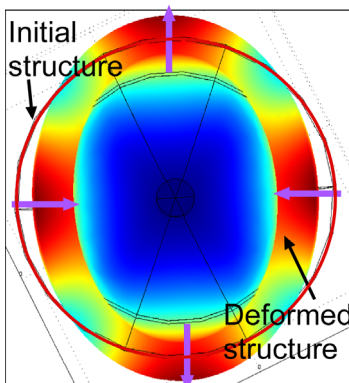


Figure 5: Simulated mode shape of the 4 node "wine glass" resonance mode. The simulated and the experimentally measured values of the resonance frequency were  $1.36$  and  $1.379 \text{ MHz}$ , respectively.

### Resonance Characteristics of Mushroom Structures

Finite element simulations were performed in order to determine the resonance frequency of the fabricated structure. Eigen frequency analysis is carried out on the mushroom-shaped structure with fixed boundary condition applied to the stem of the structure. The diameter of the stem was  $200 \mu\text{m}$  and the machining depth was assumed to be  $250 \mu\text{m}$ . Figure 5 shows the simulated mode shape of the 4-node "wine-glass" resonance mode in the mushroom structure. It consists of four anti-nodes of maximum displacement and four nodes of minimum displacement. This mode is selected as it is expected to have low anchor loss. Simulations suggest that the resonance frequency of this mode is  $1.36 \text{ MHz}$ .

The mushroom-shaped structure is actuated with a PZT stack actuator ( $5 \text{ mm} \times 5 \text{ mm} \times 2 \text{ mm}$ , Physik Instrumente Inc.). The stem of the mushroom structure is bonded to the PZT through a small brass spacer using adhesive polymer. The PZT is mounted on a high precision XY stage (CVI Melles Griot) attached to a rotary stage (Thorlabs RP01) which enables easy centering of the structure to the axis of rotation of the rotary stage. This also enables the measurement of the vibration velocity along the circumference of the mushroom-shaped resonator in order to verify the resonance mode. The vibration velocity of the mushroom-shaped structure is measured using a laser vibrometer (Polytec OFV3001S). The outer surface of the structure is sputtered with a thin layer of gold in order to provide a reflecting surface. The HP4395A network analyzer connected to a power amplifier is used to sweep the frequency of the PZT and to record the corresponding output from the laser vibrometer.

The resonance frequency of the "wine glass" mode is experimentally measured to be  $1.379 \text{ MHz}$ . This matches well with the simulation results described above. The mode shape is verified by rotating the structure on the rotary stage and measuring the vibration velocity along the

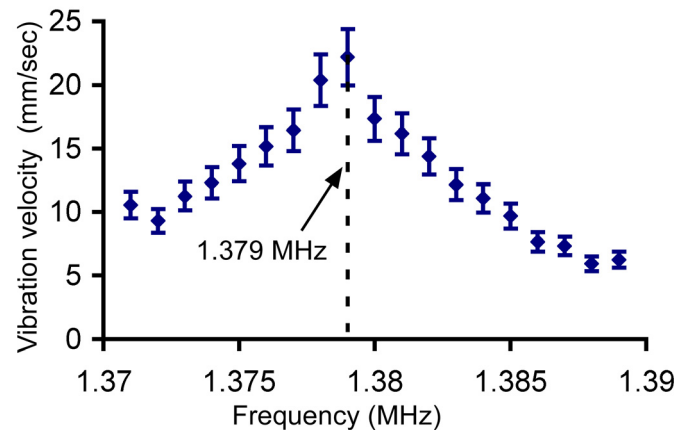


Figure 6: Resonance characteristics of mushroom-shaped structure around the 4-node wine glass mode frequency ( $1.379 \text{ MHz}$ ) in air. The quality factor of the resonance mode was experimentally measured at 345 in air, limited largely by anchor loss.

circumference. The variation in the vibration amplitude of the mushroom structure as a function of actuation frequency is also measured and the results are shown in Fig. 6. The quality factor of the resonance mode was measured to be 345 in air. The quality factor is believed to be constrained primarily by the method of attachment (adhesive polymer) to the PZT substrate.

## CONCLUSIONS

A 3D micromachining process combining batch mode micro ultrasonic machining, lapping and micro electro-discharge machining for fabrication of concave and mushroom-shaped spherical structures is described. This process is capable of machining structures with minimum internal stress from a wide variety of materials such as glass, fused quartz and ceramics. Stainless steel 440 is a suitable tool material for the ultrasonic micromachining with a tool wear below 5%. A machining rate of 24  $\mu\text{m}/\text{sec}$  is achieved for fabrication of concave and mushroom-shaped spherical structures from 1 mm diameter NBK-7 glass spheres. Finite element simulations has been performed to determine the resonance frequency of the “wine-glass” mode in the mushroom-shaped structure. The quality factor of the “wine-glass” resonance mode in the mushroom-shaped spherical structure is measured to be 345 in air. This approach has been proved feasible and bears significant promise in the long term for wafer-scale microfabrication of spherical structures from high Q materials such as fused quartz.

## ACKNOWLEDGEMENTS

The authors would like to thank Prof. Karl Grosh and Katherine Kingsley for their help with the experiments using laser vibrometer. This work was supported in part by Defense Advanced Research Projects Agency (DARPA)

## REFERENCES

- [1] A. Matthews, and F.J. Rybak, “Comparison of hemispherical resonator gyros and optical gyros,” *IEEE Aerospace and Electronic Systems Magazine*, 7, pp. 40-46, 1992.
- [2] A.M. Shkel, C. Acar and C. Painter, “Two types of micromachined vibratory gyroscopes,” *IEEE Sensors*, pp. 531-536, 2005.
- [3] E. A. Izmailov, M. M. Kolesnik, A. M. Osipov and A. V. Akimov, “Hemispherical resonator gyro technology. Problems and possible ways of their solutions,” *RTO SCI International Conference on Integrated Navigation Systems*, 1999.
- [4] E. W. Becker, W. Ehrfeld, P. Hagmann, A. Maner and D. Munchmeyer, “Fabrication of microstructures with high aspect ratios and great structural heights by synchrotron radiation lithography, galvanofarming, and plastic molding,” *Microelectronic Engineering*, 4, pp. 35-56, 1986.
- [5] H. Guckel, “High-aspect-ratio micromachining via deep X-ray lithography,” *Proceedings of the IEEE*, 86, pp. 1586-1593, 1998.
- [6] Robert Bosch GmbH, U.S. Pat. 4855017, U.S. Pat. 4784720, 1994.
- [7] T.K.A. Chou and K. Najafi, “Fabrication of out of plane curved surfaces in Si by utilizing RIE lag,” *IEEE International Conference on Micro Electro Mechanical Systems*, pp. 145-148, 2002.
- [8] K.D. Wise, M.G. Robinson, and W.J. Hillegas, “Solid-state process to produce hemispherical components for internal fusion targets,” *Journal of Vacuum Science Technology*, 16, pp. 1179-1182, 1981.
- [9] M. Zalalutdinov, K.L. Aubin, R.B. Reichenbach, A.T. Zehnder, B. Houston, J. M. Parpia and H. G. Craighead, “Shell type micromechanical actuator and resonator,” *Applied Physics Letters*, 83, pp. 3815-3817, 2003.
- [10] E.J. Eklund and A.M. Shkel, “Glass blowing on a wafer level,” *Journal of Microelectromechanical Systems*, 16, pp. 232-239, 2007.
- [11] T. Li and Y.B. Gianchandani, “A micromachining process for die-scale pattern transfer in ceramics and its application to bulk piezoelectric actuators,” *Journal of Microelectromechanical Systems*, 15, pp. 605-612, 2006.
- [12] T. Li and Y.B. Gianchandani, “A high speed batch mode ultrasonic machining technology for multi-level quartz crystal microstructures,” *IEEE International Conference on Micro Electro Mechanical Systems*, pp. 398-401, 2010.